Gustafsson, Tom; Lederer, Philip

Mixed finite elements for Bingham flow in a pipe

Published in:
Numerische Mathematik

DOI:
10.1007/s00211-022-01332-w

Published: 10/11/2022

Document Version
Publisher's PDF, also known as Version of record

Numerische Mathematik (2022) 152:819–840
https://doi.org/10.1007/s00211-022-01332-w

Numerische Mathematik

Mixed finite elements for Bingham flow in a pipe

Tom Gustafsson[1] · **Philip L. Lederer**[1]

Received: 25 May 2022 / Revised: 13 September 2022 / Accepted: 26 October 2022 /
Published online: 10 November 2022

Abstract
We consider mixed finite element approximations of viscous, plastic Bingham flow in a cylindrical pipe. A novel a priori and a posteriori error analysis is introduced which is based on a discrete mesh dependent norm for the normalized Lagrange multiplier. This allows proving stability for various conforming finite elements. Numerical examples are presented to support the theory and to demonstrate adaptive mesh refinement.

Mathematics Subject Classification 65N30 · 65N12 · 76M10

1 Introduction

In this work we consider a viscous, plastic (Bingham) fluid which behaves like a solid at low stresses and like a viscous fluid at high stresses, see [1–4] and the more recent review article [5]. An everyday example is toothpaste which extrudes from the tube as a solid plug when stress is applied, remains solid in the middle of the plug and exhibits fluid-like behavior near the tube wall. The velocity stays constant within the solid part, i.e. $\nabla u = \mathbf{0}$, and this condition is enforced using a normalized vectorial Lagrange multiplier $\boldsymbol{\lambda}$. Note that the physical stress vector is $g\boldsymbol{\lambda}$, and the shear stress is given by its length $g|\boldsymbol{\lambda}|$. Here $g > 0$ is a given fixed threshold value for the shear stress at which the solid becomes liquid when exceeded. According to Section 8 in [6] this gives the strong formulation

$$-\mu\Delta u - g\,\mathrm{div}\,\boldsymbol{\lambda} = f \quad \text{in } \Omega, \tag{1a}$$

$$\boldsymbol{\lambda}\cdot\nabla u = |\nabla u| \quad \text{in } \Omega, \tag{1b}$$

✉ Tom Gustafsson
tom.gustafsson@aalto.fi

Philip L. Lederer
philip.lederer@aalto.fi

[1] Department of Mathematics and Systems Analysis, School of Science, Aalto University, Otakaari 1 B, 00076 AALTO Espoo, Finland

$$|\boldsymbol{\lambda}| \leq 1 \quad \text{in } \Omega, \tag{1c}$$

$$u = 0 \quad \text{on } \partial\Omega, \tag{1d}$$

where μ is the viscosity of the considered fluid, and f describes the pressure drop along the pipe. Note that in practice the pressure drop is often constant over the cross section. However, in this work we assume that $f \in L^2(\Omega)$.

Several contributions in the field of Bingham-type fluid computations were made by Glowinski and collaborators; cf. [7–9]. In the latter a linear approximation was introduced and a suboptimal a priori error estimate for the velocity was given. An optimal linear convergence of some low order (mixed) methods was discussed in the works [10, 11]. Glowinski also provided an exact solution for the model problem of a circular domain with a constant load. Since even this simple geometry and loading leads to a solution that is only in $H^{5/2-\epsilon}(\Omega)$, $\epsilon > 0$, a higher regularity for general Bingham-type flows is unlikely. Due to this non-smooth nature of the problem, the use of adaptive error control seems highly desirable, see for example [12] and the references therein, and more recently in [13]. In particular, we would like to highlight the work [14] where the authors introduced the same a posteriori estimator that we derive in this work. More precisely they bound the velocity error in terms of the load, the discrete velocity u_h and the discrete approximation of the Lagrange multiplier $\boldsymbol{\lambda}_h$,

$$\|u - u_h\|_1 \lesssim \eta(f, u_h, \boldsymbol{\lambda}_h),$$

where η is some estimator. Although their definition of η is reasonable, proper error control is not guaranteed since their stability analysis does not include a bound for $\boldsymbol{\lambda}_h$. The main problem can be traced back to the lack of a Babuška–Brezzi condition for the considered linear Lagrangian velocity space and the space of element-wise vector-valued constants for the Lagrange multiplier (which is the same discretization used in [9]). As a result discrete stability for both u_h and $\boldsymbol{\lambda}_h$ is not present, i.e. the estimator η could be arbitrarily large.

The main contribution of this work is a novel stability and error analysis of a mixed finite element approximation of (1). For this we build upon the ideas from one of the authors work [15] on obstacle problems, and the corresponding references therein. Our analysis is based on proving a discrete Babuška–Brezzi condition using a mesh dependent norm; cf. [16]. This allows us to consider various finite element pairs suitable for approximating (1). Beside continuous and discrete stability (see Sects. 2 and 3) we derive an a priori error estimate and discuss linear convergence for sufficiently regular solutions in Sect. 4. Our approach then further allows deriving a residual based a posteriori error estimator (see Sect. 5) which is globally reliable and locally efficient up to a consistency term. We want to emphasize that our analysis gives full control for both the error of the velocity and the error of the (divergence of the) Lagrange multiplier. We conclude the work in Sect. 6 where we give insight on how to solve the discrete system and provide several numerical examples to validate our analysis.

2 Continuous stability

The weak formulation of (1) finds $u \in V$ and $\boldsymbol{\lambda} \in \boldsymbol{\Lambda}$ such that

$$(\mu \nabla u, \nabla v) + (g \nabla v, \boldsymbol{\lambda}) = (f, v) \quad \forall v \in V, \tag{2a}$$

$$(g \nabla u, \boldsymbol{\mu} - \boldsymbol{\lambda}) \leq 0 \quad \forall \boldsymbol{\mu} \in \boldsymbol{\Lambda}, \tag{2b}$$

where $V = H_0^1(\Omega)$ and $\boldsymbol{\Lambda} = \{\boldsymbol{\mu} \in L^2(\Omega, \mathbb{R}^2) : |\boldsymbol{\mu}| \leq 1 \text{ a.e. in } \Omega\}$; see also [8]. Combining (2a) and (2b) gives

$$(\mu \nabla u, \nabla v) + (g \nabla v, \boldsymbol{\lambda}) + (g \nabla u, \boldsymbol{\mu} - \boldsymbol{\lambda}) \leq (f, v) \tag{3}$$

for every $(v, \boldsymbol{\mu}) \in V \times \boldsymbol{\Lambda}$. Note that the solution of (3) is unique up to a divergence-free component, i.e. $\boldsymbol{\lambda} + \boldsymbol{\xi}$ is also a solution if $\operatorname{div} \boldsymbol{\xi} = 0$. For the stability analysis we choose the standard H^1-norm for the space V, and the dual norm $\|\operatorname{div}(\cdot)\|_{-1}$ for $\boldsymbol{\Lambda}$. Note that the latter is strictly speaking not a norm, but only a seminorm. Thus, all error estimates for $\boldsymbol{\lambda}$ from this work will not prove any convergence of the corresponding approximation in a strong sense, but only show convergence of its distributional divergence.

To simplify the notation we will from now on set $g = \mu = 1$. In the following we use the shorthand notation

$$\mathcal{B}(w, \boldsymbol{\xi}; v, \boldsymbol{\mu}) = (\nabla w, \nabla v) + (\nabla v, \boldsymbol{\xi}) + (\nabla w, \boldsymbol{\mu}). \tag{4}$$

Using Cauchy–Schwarz and the continuity of the duality pairing

$$(\nabla v, \boldsymbol{\xi}) = \langle \operatorname{div} \boldsymbol{\xi}, v \rangle_{-1} \leq \|v\|_1 \|\operatorname{div} \boldsymbol{\xi}\|_{-1} \quad \forall v \in V, \boldsymbol{\xi} \in \boldsymbol{Q},$$

with $\boldsymbol{Q} = L^2(\Omega, \mathbb{R}^2)$, one immediately sees that $\mathcal{B}$ is continuous, i.e. we have

$$\mathcal{B}(w, \boldsymbol{\xi}; v, \boldsymbol{\mu}) \lesssim (\|w\|_1 + \|\operatorname{div} \boldsymbol{\xi}\|_{-1})(\|v\|_1 + \|\operatorname{div} \boldsymbol{\mu}\|_{-1}). \tag{5}$$

Throughout the paper we write $a \lesssim b$ (or $a \gtrsim b$) if there exists a constant $C > 0$, independent of the finite element mesh, such that $a \leq Cb$ (or $a \geq Cb$). If $a \lesssim b$ and $b \lesssim a$ then we write $a \sim b$.

Theorem 1 *For every $(w, \boldsymbol{\xi}) \in V \times \boldsymbol{Q}$ there exists a function $r \in V$ such that*

$$\mathcal{B}(w, \boldsymbol{\xi}; r, -\boldsymbol{\xi}) \gtrsim (\|w\|_1 + \|\operatorname{div} \boldsymbol{\xi}\|_{-1})^2 \tag{6}$$

and

$$\|r\|_1 \lesssim \|w\|_1 + \|\operatorname{div} \boldsymbol{\xi}\|_{-1}. \tag{7}$$

Proof We have

$$\mathcal{B}(w, \boldsymbol{\xi}; w, -\boldsymbol{\xi}) = \|\nabla w\|_0^2. \tag{8}$$

Moreover, let $q \in V$. Then

$$\mathcal{B}(w, \boldsymbol{\xi}; q, 0) = (\nabla w, \nabla q) + (\boldsymbol{\xi}, \nabla q). \tag{9}$$

If q is chosen as the solution to

$$(\nabla q, \nabla z) = (\boldsymbol{\xi}, \nabla z) \quad \forall z \in V, \tag{10}$$

then testing with $z = q$ gives $(\boldsymbol{\xi}, \nabla q) = \|\nabla q\|_0^2$. By the definition of $\|\cdot\|_{-1}$ and Cauchy–Schwarz we have

$$\|\operatorname{div} \boldsymbol{\xi}\|_{-1} = \sup_{v \in V} \frac{(\boldsymbol{\xi}, \nabla v)}{\|v\|_1} \leq \|\nabla q\|_0. \tag{11}$$

Now choose $r := w + q$. Combining (8), (9) and (11), and applying Cauchy–Schwarz and Young's inequalities on (9) gives the first result (6).

For (7) the triangle inequality gives $\|r\|_1 \leq \|w\|_1 + \|q\|_1$. Using Friedrichs inequality we get

$$\|q\|_1^2 \lesssim \|\nabla q\|_0^2 = (\nabla q, \boldsymbol{\xi}) = \langle q, \operatorname{div} \boldsymbol{\xi}\rangle_{-1} \leq \|q\|_1 \|\operatorname{div} \boldsymbol{\xi}\|_{-1},$$

which concludes the proof. □

3 Finite element method

Let $V_h \subset V$ and $\boldsymbol{Q}_h \subset \boldsymbol{Q}$. We define the discrete subspace $\boldsymbol{\Lambda}_h \subset \boldsymbol{Q}_h$ as $\boldsymbol{\Lambda}_h = \{\boldsymbol{\mu}_h \in \boldsymbol{Q}_h : |\boldsymbol{\mu}_h| \leq 1 \text{ a.e. in } \Omega\}$. Let $\mathcal{T}_h$ be a shape regular triangulation of Ω and h_T denote the diameter of $T \in \mathcal{T}_h$. Further let $\mathcal{E}_h$ denote the set of edges with length h_E for all $E \in \mathcal{E}_h$, for which we have, due to shape regularity, $h_E \sim h_T$. The discrete norm for $\boldsymbol{\mu}_h \in \boldsymbol{\Lambda}_h$ is

$$\|\operatorname{div} \boldsymbol{\mu}_h\|_{-1,h}^2 = \sum_{T \in \mathcal{T}_h} h_T^2 \|\operatorname{div} \boldsymbol{\mu}_h\|_{0,T}^2 + \sum_{E \in \mathcal{E}_h} h_E \|[\![\boldsymbol{\mu}_h \cdot \boldsymbol{n}]\!]\|_{0,E}^2, \tag{12}$$

where $[\![\cdot]\!]$ is the usual jump operator. The discrete formulation reads: find $(u_h, \boldsymbol{\lambda}_h) \in V_h \times \boldsymbol{\Lambda}_h$ such that

$$\mathcal{B}(u_h, \boldsymbol{\lambda}_h; v_h, \boldsymbol{\mu}_h - \boldsymbol{\lambda}_h) \leq (f, v_h) \quad \forall (v_h, \boldsymbol{\mu}_h) \in V_h \times \boldsymbol{\Lambda}_h. \tag{13}$$

As in the continuous setting, we can prove stability of the mixed method (13) if the following Babuška–Brezzi condition is valid

$$\sup_{v_h \in V_h} \frac{(\boldsymbol{\xi}_h, \nabla v_h)}{\|v_h\|_1} \gtrsim \|\operatorname{div} \boldsymbol{\xi}_h\|_{-1} \quad \forall \boldsymbol{\xi}_h \in \boldsymbol{Q}_h. \tag{14}$$

Theorem 2 *Suppose V_h and $\boldsymbol{\Lambda}_h$ satisfy (14). Then for every $(w_h, \boldsymbol{\xi}_h) \in V_h \times \boldsymbol{Q}_h$ there exists a function $r_h \in V_h$ such that*

$$\mathcal{B}(w_h, \boldsymbol{\xi}_h; r_h, -\boldsymbol{\xi}_h) \gtrsim (\|w_h\|_1 + \|\operatorname{div} \boldsymbol{\xi}_h\|_{-1})^2, \tag{15}$$

and

$$\|r_h\|_1 \lesssim \|w_h\|_1 + \|\operatorname{div} \boldsymbol{\xi}_h\|_{-1}. \tag{16}$$

Proof This is similar to the proof of Theorem 1 but using (14) in the intermediate step (11). □

An explicit proof of condition (14) might be difficult depending on the choice of V_h and $\boldsymbol{Q}_h$. To this end, we show that it is sufficient to prove a discrete condition using the mesh dependent norm (12), see Theorem 3. In order to prove Theorem 3, we first consider the following preliminary result. In the following, let $\Pi_h : L^2(\Omega) \to V_h$ be the Clément quasi interpolation operator [17] with the stability and interpolation properties

$$\|\Pi_h v\|_1 \leq C_s \|v\|_1 \quad \forall v \in V, \tag{17a}$$

$$\Big(\sum_{T \in \mathcal{T}_h} h_T^{-2} \|v - \Pi_h v\|_{0,T}^2 + \sum_{E \in \mathcal{E}_h} h_E^{-1} \|v - \Pi_h v\|_{0,E}^2 \Big)^{1/2} \leq C_i \|v\|_1 \quad \forall v \in V. \tag{17b}$$

Lemma 1 *There exists constants $C_1, C_2 > 0$ such that*

$$\sup_{v_h \in V_h} \frac{(\boldsymbol{\xi}_h, \nabla v_h)}{\|v_h\|_1} \geq C_1 \|\operatorname{div} \boldsymbol{\xi}_h\|_{-1} - C_2 \|\operatorname{div} \boldsymbol{\xi}_h\|_{-1,h} \quad \forall \boldsymbol{\xi}_h \in \boldsymbol{Q}_h. \tag{18}$$

Proof Choose an arbitrary $\boldsymbol{\xi}_h \in \boldsymbol{Q}_h$. By Theorem 1 there exists a function $r \in V$ such that

$$(\boldsymbol{\xi}_h, \nabla r) \geq C' \|r\|_1 \|\operatorname{div} \boldsymbol{\xi}_h\|_{-1}.$$

Using the Clément operator we have for the difference

$$
\begin{aligned}
(\boldsymbol{\xi}_h, \nabla(\Pi_h r - r)) &= \sum_{T\in\mathcal{T}_h} (\boldsymbol{\xi}_h, \nabla(\Pi_h r - r))_T \\
&= -\sum_{T\in\mathcal{T}_h} (\operatorname{div}\boldsymbol{\xi}_h, \Pi_h r - r)_T + (\Pi_h r - r, \boldsymbol{\xi}_h\cdot\boldsymbol{n})_{\partial T} \\
&\geq -\sum_{T\in\mathcal{T}_h} h_T^{-1}\|r-\Pi_h r\|_{0,T} h_T \|\operatorname{div}\boldsymbol{\xi}_h\|_{0,T} \\
&\quad -\sum_{E\in\mathcal{E}_h} h_E \|\,[\![\boldsymbol{\xi}_h\cdot\boldsymbol{n}]\!]\,\|_{0,E} h_E^{-1}\|r-\Pi_h r\|_{0,E} \\
&\geq -2C_i\|r\|_1\|\operatorname{div}\boldsymbol{\xi}_h\|_{-1,h}.
\end{aligned}
$$

Thus, in total we have

$$
\begin{aligned}
(\boldsymbol{\xi}_h, \nabla\Pi_h r) &= (\boldsymbol{\xi}_h, \nabla(\Pi_h r - r)) + (\boldsymbol{\xi}_h, \nabla r) \\
&\geq -2C_i\|r\|_1\|\operatorname{div}\boldsymbol{\xi}_h\|_{-1,h} + C'\|r\|_1\|\operatorname{div}\boldsymbol{\xi}_h\|_{-1} \\
&\geq -C_2\|\operatorname{div}\boldsymbol{\xi}_h\|_{-1,h}\|\Pi_h r\|_1 + C_1\|\operatorname{div}\boldsymbol{\xi}_h\|_{-1}\|\Pi_h r\|_1,
\end{aligned}
$$

where $C_2 = 2C_i/C_s$ and $C_1 = C'/C_s$, which proves (18). □

Theorem 3 *If the discrete Babuška–Brezzi condition*

$$
\sup_{v_h\in V_h} \frac{(\boldsymbol{\xi}_h, \nabla v_h)}{\|v_h\|_1} \gtrsim \|\operatorname{div}\boldsymbol{\xi}_h\|_{-1,h} \quad \forall \boldsymbol{\xi}_h \in \boldsymbol{Q}_h, \tag{19}
$$

holds true, then the discrete spaces also fulfill (14).

Proof Suppose that (19) is valid with a constant $C_3 > 0$, then we have for a convex combination with $t > 0$ and using Lemma 1 that

$$
\begin{aligned}
\sup_{v_h\in V_h} \frac{(\boldsymbol{\xi}_h, \nabla v_h)}{\|v_h\|_1} &= t \sup_{v_h\in V_h} \frac{(\boldsymbol{\xi}_h, \nabla v_h)}{\|v_h\|_1} + (1-t)\sup_{v_h\in V_h} \frac{(\boldsymbol{\xi}_h, \nabla v_h)}{\|v_h\|_1} \\
&\gtrsim t(C_1\|\operatorname{div}\boldsymbol{\xi}_h\|_{-1} - C_2\|\operatorname{div}\boldsymbol{\xi}_h\|_{-1,h}) + (1-t)C_3\|\operatorname{div}\boldsymbol{\xi}_h\|_{-1,h} \\
&\gtrsim \tilde{C}\|\operatorname{div}\boldsymbol{\xi}_h\|_{-1},
\end{aligned}
$$

where we have chosen $t := \frac{1}{2}C_3(C_2+C_3)^{-1}$ and thus $\tilde{C} = C_1C_3/(2(C_2+C_3))$. □

3.1 Some stable discretizations

Theorem 3 shows that it is sufficient to prove condition (19) for some finite element spaces V_h and $\boldsymbol{Q}_h$. In the following we discuss some stable choices. Let $\mathbb{P}^l(K)$ denote the space of polynomials of order $l \geq 0$ on $K \in \mathcal{T}_h$, and let $\mathbb{P}^l(K, \mathbb{R}^2)$ denote its vector-valued version. The same notation is used for polynomials on $E \in \mathcal{E}_h$.

The $P^k P^{k-2}$ family

For $k \geq 2$, we choose the spaces

$$V_h := \{v_h \in V : v_h|_T \in \mathbb{P}^k(T)\ \forall T \in \mathcal{T}_h\}, \tag{20a}$$

$$\boldsymbol{Q}_h := \{\boldsymbol{\mu}_h \in \boldsymbol{Q} : v_h|_T \in \mathbb{P}^{k-2}(T, \mathbb{R}^2)\ \forall T \in \mathcal{T}_h\}. \tag{20b}$$

Lemma 2 *The discrete spaces defined by (20) fulfill the discrete condition (19).*

Proof Let $\boldsymbol{\xi}_h \in \boldsymbol{Q}_h$ be arbitrary. We choose $v_h \in V_h$ such that

$$v_h(x_i) = 0 \quad \forall \text{ vertices } x_i, \tag{21a}$$

$$\int_E v_h r \,\mathrm{d}s = \int_E h_E \,[\![\boldsymbol{\xi}_h \cdot \boldsymbol{n}]\!]\, r \,\mathrm{d}s \quad \forall r \in \mathbb{P}^{k-2}(E), \forall E \in \mathcal{E}_h, \tag{21b}$$

$$\int_T v_h l \,\mathrm{d}x = -\int_T h_T^2 \operatorname{div} \boldsymbol{\xi}_h l \,\mathrm{d}x \quad \forall l \in \mathbb{P}^{k-3}(T), \forall T \in \mathcal{T}_h. \tag{21c}$$

Element-wise integration by parts and using that $[\![\boldsymbol{\xi}_h \cdot \boldsymbol{n}]\!] \in \mathbb{P}^{k-2}(E)$ for all edges $E \in \mathcal{E}_h$, and $\operatorname{div} \boldsymbol{\xi}_h \in \mathbb{P}^{k-3}(T)$ for all elements $T \in \mathcal{T}_h$, we have

$$(\nabla v_h, \boldsymbol{\xi}_h) = \|\operatorname{div} \boldsymbol{\xi}_h\|_{-1,h}^2.$$

By a standard scaling argument we have on each element $T \in \mathcal{T}_h$

$$\begin{aligned} \|\nabla v_h\|_{0,T}^2 &\sim \sum_{E \subset \partial T} \frac{1}{h_E} \|v_h\|_{0,E}^2 + \frac{1}{h_T^2} \|v_h\|_{0,T}^2 \\ &\sim \sum_{E \subset \partial T} \frac{1}{h_E} \|\Pi_E^{k-2} v_h\|_{0,E}^2 + \frac{1}{h_T^2} \|\Pi_T^{k-3} v_h\|_{0,T}^2, \end{aligned} \tag{22}$$

where Π_E^{k-2} and Π_T^{k-3} are the edge-wise and element-wise L^2-projection onto polynomials of order $k-2$ and $k-3$, respectively. Note that the second equivalence follows due to v_h vanishing at all vertices, see (21a). Using this equivalence we have by the moments (21) and the Cauchy–Schwarz inequality

$$\begin{aligned} \|\nabla v_h\|_{0,T}^2 &\lesssim \sum_{E \subset \partial T} \frac{1}{h_E} \int_E (\Pi_E^{k-2} v_h)^2 \,\mathrm{d}s + \frac{1}{h_T^2} \int_T (\Pi_T^{k-3} v_h)^2 \,\mathrm{d}x \\ &= \sum_{E \subset \partial T} \int_E \Pi_E^{k-2} v_h \,[\![\boldsymbol{\xi}_h \cdot \boldsymbol{n}]\!] \,\mathrm{d}s - \int_T \Pi_T^{k-3} v_h \operatorname{div} \boldsymbol{\xi}_h \,\mathrm{d}x \\ &\lesssim \Big(\sum_{E \subset \partial T} \frac{1}{h_E} \|\Pi_E^{k-2} v_h\|_{0,E}^2 + \frac{1}{h_T^2} \|\Pi_T^{k-3} v_h\|_{0,T}^2 \Big)^{1/2} \end{aligned}$$

$$\Big(\sum_{E \subset \partial T} h_E \| [\![\boldsymbol{\xi}_h \cdot \boldsymbol{n}]\!] \|_{0,E}^2 + h_T^2 \| \operatorname{div} \boldsymbol{\xi}_h \|_{0,T}^2 \Big)^{1/2}.$$

Summing over all elements and using the norm equivalence (22) we conclude the proof.

□

The MINI family

For $k \geq 1$, we choose the spaces

$$V_h := \{ v_h \in V : v_h|_T \in \mathbb{P}^{k+2}(T) \; \forall T \in \mathcal{T}_h, \, v_h|_E \in \mathbb{P}^k(E) \; \forall E \in \mathcal{E}_h \}, \tag{23a}$$

$$\boldsymbol{Q}_h := \{ \boldsymbol{\mu}_h \in \boldsymbol{Q} : v_h|_T \in \mathbb{P}^k(T, \mathbb{R}^2) \; \forall T \in \mathcal{T}_h \} \cap H^1(\Omega, \mathbb{R}^2). \tag{23b}$$

Note that since now $\boldsymbol{Q}_h$ is a subset of $H^1(\Omega, \mathbb{R}^2)$, the normal jumps in $\| \operatorname{div}(\cdot) \|_{-1,h}$ vanish.

Lemma 3 *The discrete spaces defined by (23) fulfill the discrete condition (19).*

Proof Let $\boldsymbol{\xi}_h \in \boldsymbol{Q}_h$ be arbitrary. We choose $v_h \in V_h$ such that it vanishes at all vertices and all edges, i.e. $v_h \in H_0^1(T)$ for all elements $T \in \mathcal{T}_h$. In addition v_h fulfills

$$\int_T v_h l \, \mathrm{d}x = - \int_T h_T^2 \operatorname{div} \boldsymbol{\xi}_h l \, \mathrm{d}x \qquad \forall l \in \mathbb{P}^{k-1}(T), \forall T \in \mathcal{T}_h.$$

Using integration by parts and the fact that $\operatorname{div} \boldsymbol{\xi}_h \in \mathbb{P}^{k-1}(T)$ for all elements $T \in \mathcal{T}_h$, we have again

$$(\nabla v_h, \boldsymbol{\xi}_h) = \| \operatorname{div} \boldsymbol{\xi}_h \|_{-1,h}^2.$$

With similar scaling arguments as in the proof of Lemma 2 we also have $\| \nabla v_h \|_0 \lesssim \| \operatorname{div} \boldsymbol{\xi}_h \|_{-1,h}$, which concludes the proof. □

Remark 1 *The Crouzeix–Raviart method.* The last method we want to mention is using a nonconforming approximation of the velocity. We define the spaces

$$\begin{aligned} V_h := \{ & v_h \in L^2(\Omega, \mathbb{R}) : v_h|_T \in \mathbb{P}^1(T) \; \forall T \in \mathcal{T}_h, \\ & v_h \text{ is continuous and vanishes at midpoints} \\ & \text{of interior and boundary edges, respectively} \}, \\ \boldsymbol{Q}_h := \{ & \boldsymbol{\mu}_h \in L^2(\Omega, \mathbb{R}^2) : v_h|_T \in \mathbb{P}^0(T, \mathbb{R}^2) \; \forall T \in \mathcal{T}_h \}. \end{aligned}$$

Since the degrees-of-freedom of the velocity are again associated to edges, the stability analysis is similar as for the $P^2 P^0$ method. Further note that since $\nabla v_h \in \boldsymbol{Q}_h$ locally on

each element, one can reformulate the mixed method (13) as a primal method (without the Lagrange multiplier $\boldsymbol{\lambda}_h$) which is similar to the nonconforming approximations from [10] and (as explained in [10]) the method in [11]. Due to the extensive analysis therein, we do not consider this method in the present work, but want to mention that our techniques can be applied accordingly.

4 A priori error analysis

In this section we present an a priori error estimate and prove a linear convergence for H^2-regular velocity solutions. This stands in contrast to the suboptimal result $\mathcal{O}(h^{1/2})$ (for a linear approximation) from [7, 9] and is in accordance to the linear convergence results from [10, 11]. Although the analysis could be extended to provide a better rate for smooth solutions, a higher regularity can not be expected for Bingham-type flows as discussed in the introduction.

Theorem 4 *Let $(u_h, \boldsymbol{\lambda}_h) \in V_h \times \boldsymbol{\Lambda}_h$ be the solution of (13), then for any $(w_h, \boldsymbol{\xi}_h) \in V_h \times \boldsymbol{Q}_h$ it holds*

$$\begin{aligned}\|u - u_h\|_1 + \|\operatorname{div}(\boldsymbol{\lambda} - \boldsymbol{\lambda}_h)\|_{-1} \\ \lesssim \|u - w_h\|_1 + \|\operatorname{div}(\boldsymbol{\lambda} - \boldsymbol{\xi}_h)\|_{-1} + \sqrt{(\nabla u, \boldsymbol{\lambda} - \boldsymbol{\xi}_h)}.\end{aligned}$$

Proof Let $(w_h, \boldsymbol{\xi}_h) \in V_h \times \boldsymbol{Q}_h$ be arbitrary. By the discrete stability, see Theorem 2, we find v_h such that

$$\begin{aligned}\Big(\|u_h - w_h\|_1 + \|\operatorname{div}(\boldsymbol{\lambda}_h - \boldsymbol{\xi}_h)\|_{-1}\Big)^2 &\lesssim \mathcal{B}(u_h - w_h, \boldsymbol{\lambda}_h - \boldsymbol{\xi}_h; v_h, \boldsymbol{\xi}_h - \boldsymbol{\lambda}_h) \\ &\leq (f, v_h) - \mathcal{B}(w_h, \boldsymbol{\xi}_h; v_h, \boldsymbol{\xi}_h - \boldsymbol{\lambda}_h).\end{aligned}$$

Using the continuous problem (3) we get

$$\begin{aligned}&(f, v_h) - \mathcal{B}(w_h, \boldsymbol{\xi}_h; v_h, \boldsymbol{\xi}_h - \boldsymbol{\lambda}_h) \\ &= (\nabla u, \boldsymbol{\lambda}_h - \boldsymbol{\xi}_h) + \mathcal{B}(u - w_h, \boldsymbol{\lambda} - \boldsymbol{\xi}_h; v_h, \boldsymbol{\xi}_h - \boldsymbol{\lambda}_h) \\ &\leq (\nabla u, \boldsymbol{\lambda} - \boldsymbol{\xi}_h) + \mathcal{B}(u - w_h, \boldsymbol{\lambda} - \boldsymbol{\xi}_h; v_h, \boldsymbol{\xi}_h - \boldsymbol{\lambda}_h),\end{aligned}$$

which concludes the proof with the continuity of $\mathcal{B}$, see (5), and

$$\begin{aligned}&\|u - u_h\|_1 + \|\operatorname{div}(\boldsymbol{\lambda} - \boldsymbol{\lambda}_h)\|_{-1} \\ &\leq \|u - w_h\|_1 + \|\operatorname{div}(\boldsymbol{\lambda} - \boldsymbol{\xi}_h)\|_{-1} + \|u_h - w_h\|_1 + \|\operatorname{div}(\boldsymbol{\lambda}_h - \boldsymbol{\xi}_h)\|_{-1}.\end{aligned}$$

□

The following lemma shows that we can expect a linear convergence whenever the solution is at least H^2-regular. Note that it is essential to bound the error just in terms

of $\operatorname{div}\boldsymbol{\lambda}$, since our analysis does not provide any control for the divergence-free part of $\boldsymbol{\lambda}$. According to [7] we further have for a convex domain and a smooth soulution the stability estimate

$$|u|_2 + \|\operatorname{div}\boldsymbol{\lambda}\|_0 \lesssim \|f\|_0.$$

Lemma 4 *Let Ω be simply connected and convex. Choose V_h and $\boldsymbol{Q}_h$ as in Sect. 3.1, and let $(u_h, \boldsymbol{\lambda}_h) \in V_h \times \boldsymbol{\Lambda}_h$ be the corresponding discrete solution. Further let $u \in V \cap H^2(\Omega)$ and $\boldsymbol{\lambda} \in \boldsymbol{\Lambda} \cap H(\operatorname{div}, \Omega)$. Then there holds*

$$\|u - u_h\|_1 + \|\operatorname{div}(\boldsymbol{\lambda} - \boldsymbol{\lambda}_h)\|_{-1} \lesssim h(|u|_2 + \|\operatorname{div}\boldsymbol{\lambda}\|_0) \lesssim h\|f\|_0,$$

where $h = \max_{T\in\mathcal{T}_h} \operatorname{diam}(T)$.

Proof We solve the Dirichlet problem: find $\theta \in H_0^1(\Omega)$ such that

$$(\nabla\theta, \nabla v) = (\operatorname{div}\boldsymbol{\lambda}, v) \quad \forall v \in H_0^1(\Omega),$$

for which we have due to the assumptions on the domain that $|\theta|_2 \lesssim \|\operatorname{div}\boldsymbol{\lambda}\|_0$. Further, since $\boldsymbol{\lambda} - \nabla\theta$ is divergence free (by construction) Theorem 3.1 in [18] shows that there exists a $\phi \in H^1(\Omega)$ such that $\boldsymbol{\lambda} = \nabla\theta + \mathbf{curl}\,\phi$.

Let $w_h := I_{\mathcal{L}}u$, where $I_{\mathcal{L}}$ is the Lagrange interpolation operator onto V_h, then by the approximation properties of $I_{\mathcal{L}}$ we have

$$\|u - w_h\|_1 \lesssim h|u|_2.$$

Using integration by parts and that $\mathbf{curl}\,\nabla v = 0$ for all $v \in V$ we have

$$\|\operatorname{div}(\boldsymbol{\lambda} - \boldsymbol{\xi}_h)\|_{-1} = \sup_{v\in V} \frac{(\boldsymbol{\lambda} - \boldsymbol{\xi}_h, \nabla v)}{\|v\|_1} = \sup_{v\in V} \frac{(\boldsymbol{\lambda} - \mathbf{curl}\,\phi - \boldsymbol{\xi}_h, \nabla v)}{\|v\|_1}.$$

For the $P^k P^{k-2}$ family we choose $\boldsymbol{\xi}_h = \Pi_0\nabla\theta$, then

$$(\boldsymbol{\lambda} - \mathbf{curl}\,\phi - \boldsymbol{\xi}_h, \nabla v) = ((\mathrm{id} - \Pi_0)\nabla\theta, \nabla v) \lesssim h|\theta|_2\|\nabla v\|_0 \lesssim h\|\operatorname{div}\boldsymbol{\lambda}\|_0\|\nabla v\|_0.$$

It remains to bound the last term. For this note that since $\mathrm{id} - \Pi_0$ is orthogonal on constants we have with similar steps as above

$$(\nabla u, \boldsymbol{\lambda} - \boldsymbol{\xi}_h) = (\nabla u, (\mathrm{id} - \Pi_0)\nabla\theta) = ((\mathrm{id} - \Pi_0)\nabla u, (\mathrm{id} - \Pi_0)\nabla\theta) \lesssim h|u|_2 h\|\operatorname{div}\boldsymbol{\lambda}\|_0,$$

from which we conclude the proof.

For the MINI family, we use the same steps as above, but choose $\boldsymbol{\xi}_h = \Pi_h\nabla\theta$. Using Theorem 2.6 from [19] we get again the bound

$$(\nabla u, \boldsymbol{\lambda} - \boldsymbol{\xi}_h) \lesssim h|u|_2 h\|\operatorname{div}\boldsymbol{\lambda}\|_0,$$

and we conclude the proof with Theorem 4. □

5 A posteriori error analysis

Since a high regularity of the solution cannot be expected in general, this section is dedicated to a posteriori error control, enabling the use of adaptive mesh refinement. We define the local error estimators – including the dependency on g and μ to allow for a direct implementation – as

$$\begin{aligned}\eta_T^2 &:= h_T^2 \|\mu \Delta u_h + g \operatorname{div} \boldsymbol{\lambda}_h + f\|_{0,T}^2,\\ \eta_E^2 &:= h_E \| [\![(\mu \nabla u_h + g\boldsymbol{\lambda}_h) \cdot \boldsymbol{n}]\!] \|_{0,E}^2,\\ \eta_{\mathrm{con},T}^2 &:= g \int_T (|\nabla u_h| - \boldsymbol{\lambda}_h \cdot \nabla u_h)\, \mathrm{d}x,\end{aligned}$$

and the global estimator

$$\eta := \sqrt{\sum_{T\in\mathcal{T}_h} \eta_T^2 + \sum_{E\in\mathcal{E}_h} \eta_E^2 + \sum_{T\in\mathcal{T}_h} \eta_{\mathrm{con},T}^2}.$$

The element and edge estimators η_T and η_E, respectively, are standard residual estimators as known from the literature. The additional term $\eta_{\mathrm{con},T}$ can be interpreted as a consistency estimator of Eq. (1b). Further we want to emphasize that all estimators only depend on the distributional divergence of $\boldsymbol{\lambda}_h$ for which we have discrete stability, see Theorem 2. While this is clear for η_T and η_E, through integration by parts this is also evident for $\eta_{\mathrm{con},T}$.

Theorem 5 *There holds the a posteriori error estimate*

$$\|u - u_h\|_1 + \|\operatorname{div}(\boldsymbol{\lambda} - \boldsymbol{\lambda}_h)\|_{-1} \lesssim \eta.$$

Proof Using the continuous stability we find $v \in V$ such that

$$\begin{aligned}&(\|u - u_h\|_1 + \|\operatorname{div}(\boldsymbol{\lambda} - \boldsymbol{\lambda}_h)\|_{-1})^2\\ &\lesssim \mathcal{B}(u - u_h, \boldsymbol{\lambda} - \boldsymbol{\lambda}_h; v, \boldsymbol{\lambda}_h - \boldsymbol{\lambda})\\ &= (\nabla(u - u_h), \nabla v) + (\nabla v, \boldsymbol{\lambda} - \boldsymbol{\lambda}_h) + (\nabla(u - u_h), \boldsymbol{\lambda}_h - \boldsymbol{\lambda}),\end{aligned}$$

and $\|v\|_1 \lesssim \|u - u_h\|_1 + \|\operatorname{div}(\boldsymbol{\lambda} - \boldsymbol{\lambda}_h)\|_{-1}$. We continue with the first two terms. Using the Clément operator we have

$$(\nabla u_h, \nabla \Pi_h v) + (\nabla \Pi_h v, \boldsymbol{\lambda}_h) = (f, \Pi_h v) = (\nabla u, \nabla \Pi_h v) + (\nabla \Pi_h v, \boldsymbol{\lambda}),$$

and thus

$$(\nabla(u - u_h), \nabla v) + (\nabla v, \boldsymbol{\lambda} - \boldsymbol{\lambda}_h)$$

$$= (\nabla(u-u_h), \nabla(v-\Pi_h v)) + (\nabla(v-\Pi_h v), \boldsymbol{\lambda}-\boldsymbol{\lambda}_h)$$
$$= \sum_{T\in\mathcal{T}_h} (\nabla(u-u_h), \nabla(v-\Pi_h v))_T + (\nabla(v-\Pi_h v), \boldsymbol{\lambda}-\boldsymbol{\lambda}_h)_T.$$

Since $\operatorname{div}(-\nabla u-\boldsymbol{\lambda}) = f$, see (1a), and $f \in L^2(\Omega)$, we have that $\nabla u+\boldsymbol{\lambda} \in H(\operatorname{div}, \Omega)$, i.e. it is normal continuous. By that we have with integration by parts on each element

$$(\nabla(u-u_h), \nabla v) + (\nabla v, \boldsymbol{\lambda}-\boldsymbol{\lambda}_h)$$
$$= \sum_{T\in\mathcal{T}_h} (f + \Delta u_h + \operatorname{div}\boldsymbol{\lambda}_h, v-\Pi_h v)_T + \sum_{E\in\mathcal{E}_h} (\llbracket(\nabla u_h + \boldsymbol{\lambda}_h)\cdot\boldsymbol{n}\rrbracket, v-\Pi_h v)_E.$$

Using the properties of Π_h, cf. (17), we finally arrive at

$$(\nabla(u-u_h), \nabla v) + (\nabla v, \boldsymbol{\lambda}-\boldsymbol{\lambda}_h) \lesssim \Big(\sum_{T\in\mathcal{T}_h} \eta_T^2 + \sum_{E\in\mathcal{E}_h} \eta_E^2\Big)^{1/2} \|v\|_1.$$

It remains to bound the other term. For this note that (2b) gives $(\nabla u, \boldsymbol{\lambda}_h) \le (\nabla u, \boldsymbol{\lambda})$, and thus as $|\boldsymbol{\lambda}| \le 1$,

$$(\nabla(u-u_h), \boldsymbol{\lambda}_h-\boldsymbol{\lambda}) \le (\nabla u_h, \boldsymbol{\lambda}-\boldsymbol{\lambda}_h) \le \sum_{T\in\mathcal{T}_h} \int_T (|\nabla u_h||\boldsymbol{\lambda}| - \nabla u_h\cdot\boldsymbol{\lambda}_h)\,\mathrm{d}x$$
$$\le \sum_{T\in\mathcal{T}_h} \int_T (|\nabla u_h| - \nabla u_h\cdot\boldsymbol{\lambda}_h)\,\mathrm{d}x,$$

which concludes the proof. □

Theorem 6 and Lemma 5 below provide local and global efficiency estimates, respectively, for the residual based estimators η_T and η_E. The proofs follow with similar steps as in [15], i.e. we will provide all details of the local efficiency but refer to [15] for the proof of Lemma 5. Further note that similarly as in [15] it is not possible to provide an upper bound for the consistency error $\eta_{\mathrm{con},T}$.

For the efficiency estimates we need some additional notation. Let $\omega \subset \Omega$ be arbitrary then we define for all $\boldsymbol{\mu} \in \boldsymbol{\Lambda}$ the local dual norm by

$$\|\operatorname{div}\boldsymbol{\mu}\|_{-1,\omega} := \sup_{v\in H_0^1(\omega)} \frac{\langle v, \operatorname{div}\boldsymbol{\mu}\rangle_{-1,\omega}}{\|v\|_{1,\omega}} = \sup_{v\in H_0^1(\omega)} \frac{(\nabla v, \boldsymbol{\mu})_\omega}{\|v\|_{1,\omega}}.$$

The subset ω will be either an element $T \in \mathcal{T}_h$ or ω_E, where ω_E denotes the edge-patch for a given edge $E \in \mathcal{E}_h$. Finally, let $f_h := \Pi^q f$ be the element-wise L^2 projection onto $\mathbb{P}^q(K)$ where q is the polynomial order of the space $\boldsymbol{Q}_h$, and let

$$\operatorname{osc}_T(f) := h_T\|f-f_h\|_{0,T} \quad \text{and} \quad \operatorname{osc}(f) := \Big(\sum_{T\in\mathcal{T}_h} h_T^2\|f-f_h\|_{0,T}^2\Big)^{1/2}.$$

Theorem 6 *Let $v_h \in V_h$ and $\boldsymbol{\mu}_h \in \boldsymbol{\Lambda}_h$ be arbitrary. There holds the local efficiency*

$$h_T \|\Delta v_h + \operatorname{div} \boldsymbol{\mu}_h + f\|_{0,T} \lesssim \|u - v_h\|_{1,T} + \|\operatorname{div}(\boldsymbol{\lambda} - \boldsymbol{\mu}_h)\|_{-1,T} + \operatorname{osc}_T(f),$$
$$h_E^{1/2} \| [\![(\nabla v_h + \boldsymbol{\mu}_h) \cdot \boldsymbol{n}]\!] \|_{0,E}^2 \lesssim \|u - v_h\|_{1,\omega_E} + \|\operatorname{div}(\boldsymbol{\lambda} - \boldsymbol{\mu}_h)\|_{-1,\omega_E} + \sum_{T \subset \omega_E} \operatorname{osc}_T(f).$$

Proof The proof commences with the usual localizing technique by means of a element-wise qubic bubble function b_T. We define the localized error on T by

$$\delta_T|_T := h_T^2 b_T (\Delta v_h + \operatorname{div} \boldsymbol{\mu}_h + f_h),$$

and $\delta_T = 0$ on $\Omega \setminus T$. Since b_T vanishes on the element boundary we have that $\delta_T \in V$. Using the norm equivalence for polynomial spaces we then have

$$\begin{aligned}
&h_T^2 \|\Delta v_h + \operatorname{div} \boldsymbol{\mu}_h + f_h\|_{0,T}^2 \\
&\lesssim h_T^2 \|b_T^{1/2} (\Delta v_h + \operatorname{div} \boldsymbol{\mu}_h + f_h)\|_{0,T}^2 \\
&= (\Delta v_h + \operatorname{div} \boldsymbol{\mu}_h + f_h, \delta_T)_T \\
&= (\Delta v_h + \operatorname{div} \boldsymbol{\mu}_h, \delta_T)_T + (f, \delta_T)_T + (f_h - f, \delta_T)_T \\
&= (\Delta v_h + \operatorname{div} \boldsymbol{\mu}_h, \delta_T)_T + (-\Delta u, \delta_T)_T - \langle \operatorname{div} \boldsymbol{\lambda}, \delta_T \rangle_{-1,T} + (f_h - f, \delta_T)_T,
\end{aligned}$$

and, with integration by parts also

$$\begin{aligned}
&h_T^2 \|\Delta v_h + \operatorname{div} \boldsymbol{\mu}_h + f_h\|_{0,T}^2 \\
&\lesssim (\nabla(v_h - u), \nabla \delta_T)_T + \langle \operatorname{div}(\boldsymbol{\mu}_h - \boldsymbol{\lambda}), \delta_T \rangle_{-1,T} + (f_h - f, \delta_T)_T. \qquad (24)
\end{aligned}$$

By the inverse inequality for polynomials we have

$$\|\delta_T\|_{1,T} \lesssim h_T^{-1} \|\delta_T\|_{0,T} \sim h_T \|\Delta v_h + \operatorname{div} \boldsymbol{\mu}_h + f_h\|_{0,T}, \qquad (25)$$

and thus, with Cauchy–Schwarz inequality we derive the first estimate with

$$\begin{aligned}
&h_T^2 \|\Delta v_h + \operatorname{div} \boldsymbol{\mu}_h + f_h\|_{0,T}^2 \\
&\lesssim \|u - v_h\|_{1,T} \|\delta_T\|_{1,T} + \|\operatorname{div}(\boldsymbol{\lambda} - \boldsymbol{\mu}_h)\|_{-1,T} \|\delta_T\|_{1,T} + \operatorname{osc}_T(f) h_T^{-1} \|\delta_T\|_{0,T}.
\end{aligned}$$

For the other term we proceed similarly. For this let $\delta_E := b_E \mathcal{E}([\![(\nabla v_h + \boldsymbol{\mu}_h) \cdot \boldsymbol{n}]\!])$ where $\mathcal{E}$ is the well known extension operator onto $H_0^1(\omega_E)$, see [20], and b_E is the quadratic edge bubble. Scaling arguments and the Poincaré inequality give

$$\| [\![(\nabla v_h + \boldsymbol{\mu}_h) \cdot \boldsymbol{n}]\!] \|_{0,E} \sim h_E^{-1/2} \|\delta_E\|_{0,E} \sim h_E \|\delta_E\|_{1,\omega_E}.$$

With the same steps as for the volume term we derive the estimate

$$\begin{aligned}
\| [\![(\nabla v_h + \boldsymbol{\mu}_h) \cdot \boldsymbol{n}]\!] \|_{0,E}^2 \lesssim &(\Delta v_h + \operatorname{div} \boldsymbol{\mu}_h + f, \delta_E)_{\omega_E} \\
&+ (\nabla(v_h - u), \delta_E)_{\omega_E} + \langle \operatorname{div}(\boldsymbol{\mu}_h - \boldsymbol{\lambda}), \delta_E \rangle_{-1,\omega_E}, \qquad (26)
\end{aligned}$$

from which we conclude the proofs using the Cauchy–Schwarz inequality, the estimates of the volume term from before and (25). □

Lemma 5 *Let $v_h \in V_h$ and $\boldsymbol{\mu}_h \in \boldsymbol{\Lambda}_h$ be arbitrary. There holds the global efficiency*

$$\Big(\sum_{T \in Th} h_T^2 \| \Delta v_h + \operatorname{div} \boldsymbol{\mu}_h + f \|_{0,T}^2 \Big)^{1/2} \lesssim \| u - v_h \|_1 + \| \operatorname{div} (\boldsymbol{\lambda} - \boldsymbol{\mu}_h) \|_{-1} + \operatorname{osc}(f),$$

$$\Big(\sum_{E \in \mathcal{E}_h} h_E \| [\![(\nabla v_h + \boldsymbol{\mu}_h) \cdot \boldsymbol{n}]\!] \|_{0,E}^2 \Big)^{1/2} \lesssim \| u - v_h \|_1 + \| \operatorname{div} (\boldsymbol{\lambda} - \boldsymbol{\mu}_h) \|_{-1} + \operatorname{osc}(f).$$

Proof The proof follows with the same steps as in [15] using the intermediate estimates (26) and (24). □

6 Numerical examples

We apply an iterative algorithm to approximate the solution of the discrete problem (13). It is based on a reformulation of the inequality constraint (2b) as

$$\boldsymbol{\lambda} - \boldsymbol{P}(\boldsymbol{\lambda} + \rho \nabla u) = \mathbf{0}, \quad \rho > 0, \tag{27}$$

where $\boldsymbol{P}(\boldsymbol{\mu}) = \frac{\boldsymbol{\mu}}{\max(1, |\boldsymbol{\mu}|)}$ scales any vectors of $\mathbb{R}^2$ to maximum length one, cf. [7, 8] for discussion on similar algorithms and proofs of their convergence. The reformulation is based on the fact that $\boldsymbol{\lambda}_h$ in

$$(\boldsymbol{\xi}_h - \boldsymbol{\lambda}_h, \boldsymbol{\mu}_h - \boldsymbol{\lambda}_h) \leq 0 \quad \forall \boldsymbol{\mu}_h \in \boldsymbol{\Lambda}_h,$$

is the orthogonal projection of $\boldsymbol{\xi}_h \in \boldsymbol{Q}_h$ onto $\boldsymbol{\Lambda}_h$, and the orthogonal projection is alternatively characterized by $\boldsymbol{P}$ [8, Section 3].

Algorithm 1 (Uzawa iteration) Let $(u_h^0, \boldsymbol{\lambda}_h^0) \in V_h \times \boldsymbol{\Lambda}_h$ be an initial guess, TOL a given tolerance and set $i = 1$

1. Solve u_h^i from $(\mu \nabla u_h^i, \nabla v_h) = (f, v_h) - g(\boldsymbol{\lambda}_h^{i-1}, \nabla v_h)$ for every $v_h \in V_h$.
2. Calculate $\boldsymbol{\lambda}_h^i = \boldsymbol{P}(\boldsymbol{\lambda}_h^{i-1} + \rho \pi_h \nabla u_h^i)$ where $\pi_h : \boldsymbol{Q} \to \boldsymbol{Q}_h$ is the L^2 projection onto $\boldsymbol{Q}_h$.
3. Stop if $\| \nabla (u_h^i - u_h^{i-1}) \|_0 / \| \nabla u_h^{i-1} \|_0 < TOL$. If not, increment i and go to step (1).

We first attempt to approximate an analytical solution on a circle $\Omega = \{(x, y) \in \mathbb{R}^2 : x^2 + y^2 < R^2\}$ using uniform mesh refinements; see Fig. 1 for the sequence of meshes. For constant loading f, the coincidence set is a smaller circle with the radius $R_p = 2g/f$. The analytical solution reads $u(r) = \frac{R-r}{2}(\frac{f}{2}(R + r) - 2g)$ when $r > R_p$ and is equal to the constant $u(R_p)$ when $r \leq R_p$. Substituting the above expression into the strong formulation (1a) we find also an analytical expression for the divergence of $\boldsymbol{\lambda}$.

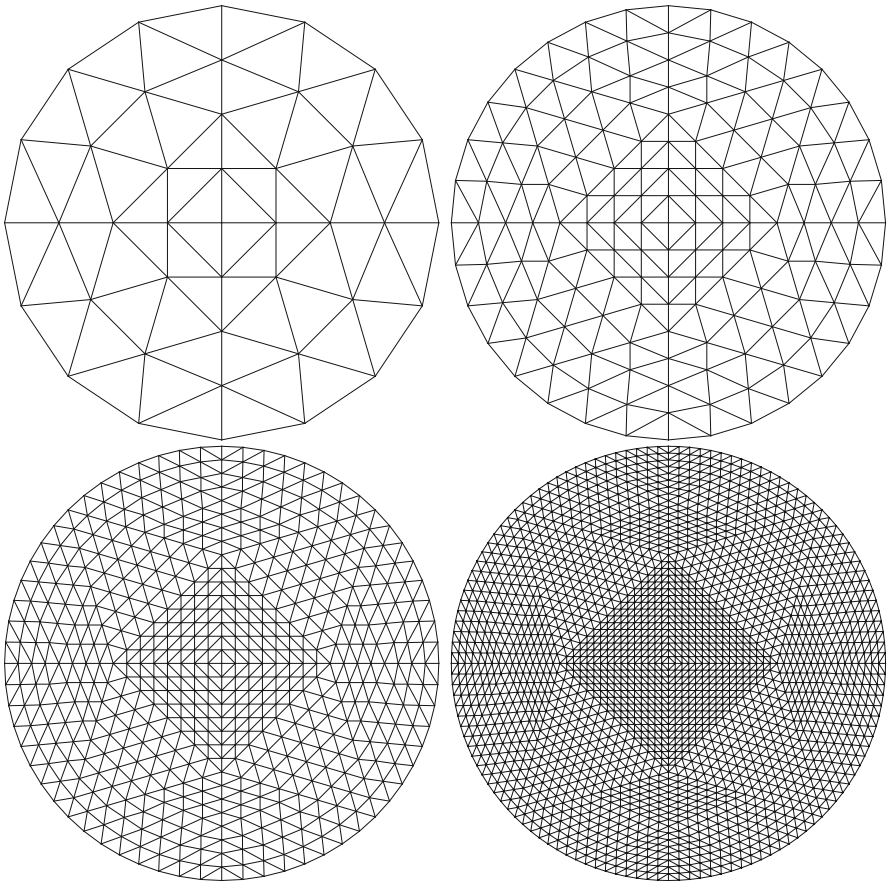

Fig. 1 The sequence of uniformly refined meshes for the convergence study

The error of the different components of the discrete norm are given in Fig. 2 with $TOL = 10^{-7}$, $R = 1$, $g = 0.1$, $f = 0.5$ and $\rho = 10$ in accordance to the suggestion in [8, Remark 3]. We observe that for the MINI and P^2P^0 methods all components converge at least linearly whereas for P^3P^1 method the H^1 seminorm of $u - u_h$ is approximately $\mathcal{O}(h^{1.7})$ and the discrete norm of $\boldsymbol{\lambda} - \boldsymbol{\lambda}_h$ is approximately $\mathcal{O}(h^{1.6})$, i.e. less than the quadratic convergence order that interpolation estimates would imply for a completely smooth solution.

Next, our aim is to improve the convergence rate with respect to the total number of degrees-of-freedom N using mesh adaptivity. We use an adaptive mesh sequence based on the a posteriori estimate of Sect. 5. An element-wise error estimator E_T is given by

$$E_T^2 = \eta_T^2 + \sum_{\substack{E \in \mathcal{E}_h, \\ E \cap \partial T \neq \emptyset}} (\tfrac{1}{2}\eta_E)^2 + \eta_{\mathrm{con},T}^2,$$

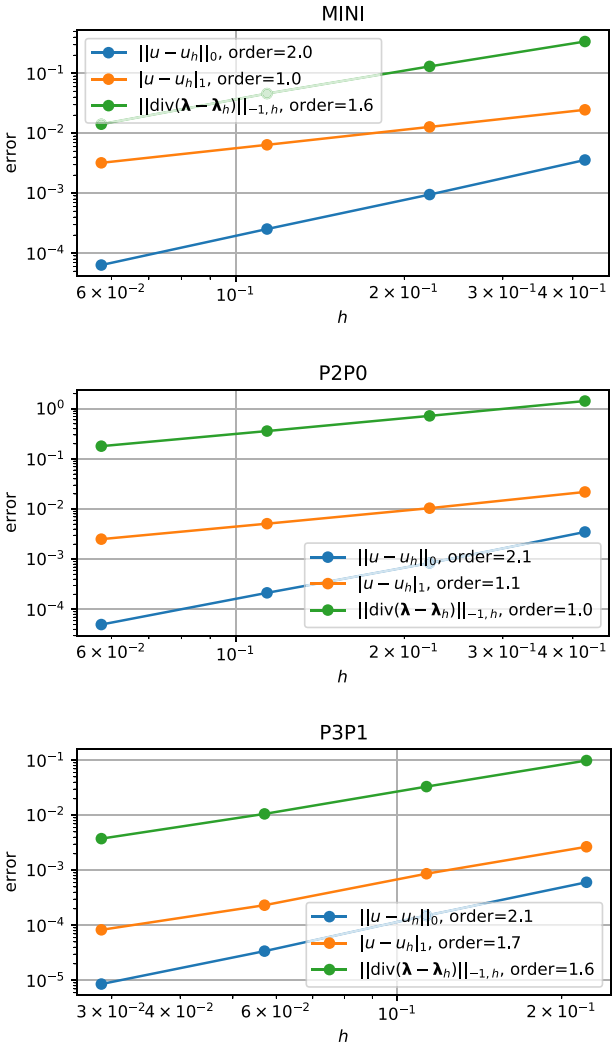

Fig. 2 Error in the different components of the discrete norm for the circle problem as a function of the mesh parameter h using the uniform mesh sequence

and we split $T' \in \mathcal{T}_h$ if

$$E_{T'} > 0.5 \max_{T \in \mathcal{T}_h} E_T.$$

The mesh is refined using the red-green-blue refinement strategy and Laplacian smoothing is applied on the refined mesh to improve its shape regularity. Some examples from the sequence of adaptive meshes are given in Fig. 3. A comparison of the error between the uniform and adaptive mesh sequences is given in Fig. 4. In particular, we observe that while the convergence rate of the error is ultimately dictated by the

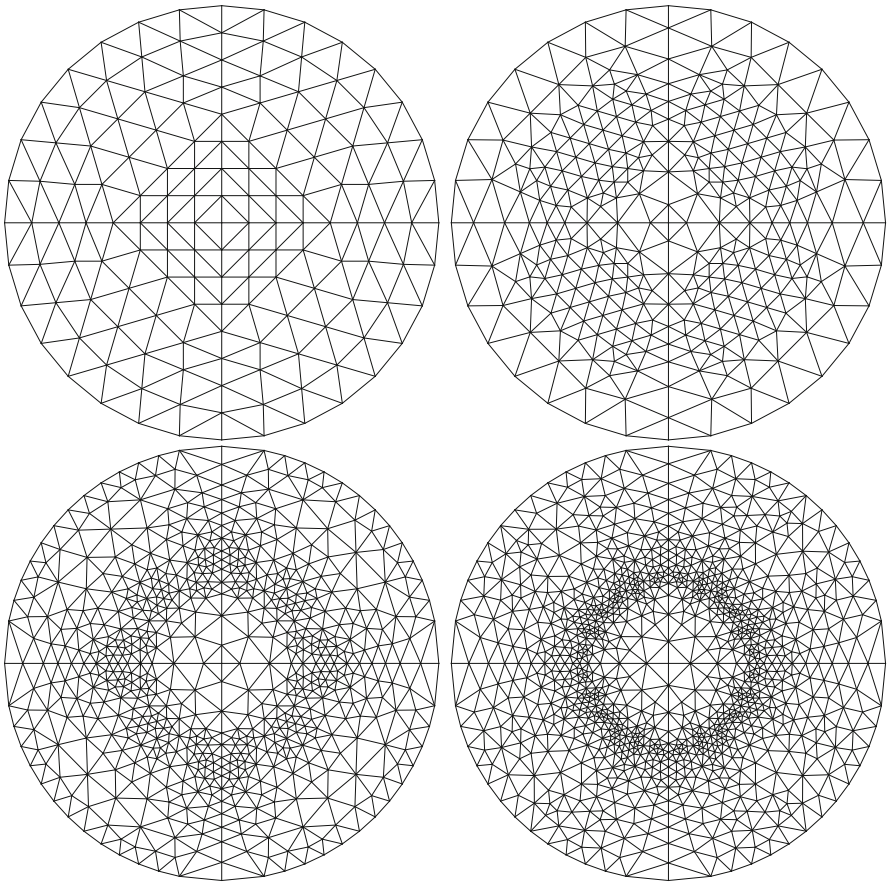

Fig. 3 Some examples from the sequence of adaptively refined meshes for the circle problem

largest component of the discrete norm (i.e. $\|\boldsymbol{\lambda} - \boldsymbol{\lambda}_h\|_{-1,h}$), there is a visible improvement in all of the components and, as a conclusion, the quadratic rate is recovered with respect to the number of degrees-of-freedom.

Finally, we consider an example in a square domain $\Omega = (0, 1)^2$ with $f = 3.6$, $g = 1.25$, $\rho = 1.5$, and no analytical solution; cf. [14, 21] for similar examples. Some meshes from the adaptive sequence and the total error estimators are given in Fig. 5. The final discrete solution is depicted in Fig. 6. As before, we observe the adaptive refinement focusing on the interfaces between the liquid and solid regions. Moreover, the estimators successfully locate and refine the so-called stagnating regions at corners of the square.

Remark 2 We used a quadratic representation of the circle boundary in order to neglect the effect of inexact geometry representation.

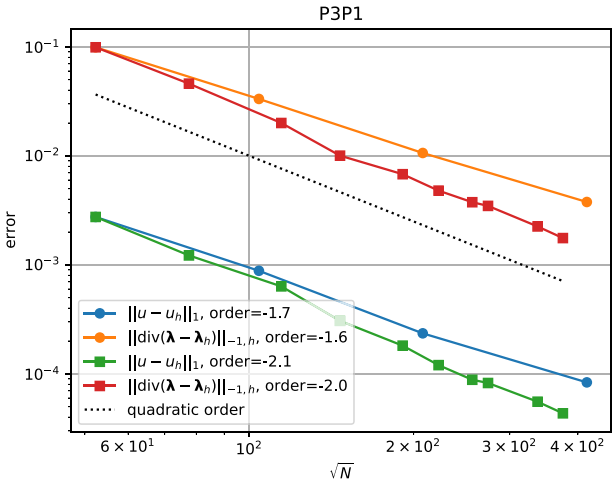

Fig. 4 Error in the different components of the discrete norm for the circle problem using P^3P^1 method. The horizontal axis is the square root of the total number of degrees-of-freedom N. A comparison is made between the uniform mesh sequence (circles) and the adaptive mesh sequence (squares)

Remark 3 We found the following equivalent form of the estimator $\eta_{\mathrm{con},T}$ to be more robust against numerical tolerances in Algorithm 1:

$$g \int_T (|\nabla u_h| - \boldsymbol{P}(\boldsymbol{\lambda}_h + \rho \pi_h \nabla u_h) \cdot \pi_h \nabla u_h) \, \mathrm{d}x.$$

Remark 4 We consider methods only up to a linear Lagrange multiplier because for a higher order method, in general, $\boldsymbol{\lambda}_h \notin \boldsymbol{\Lambda}_h$ when using Algorithm 1.

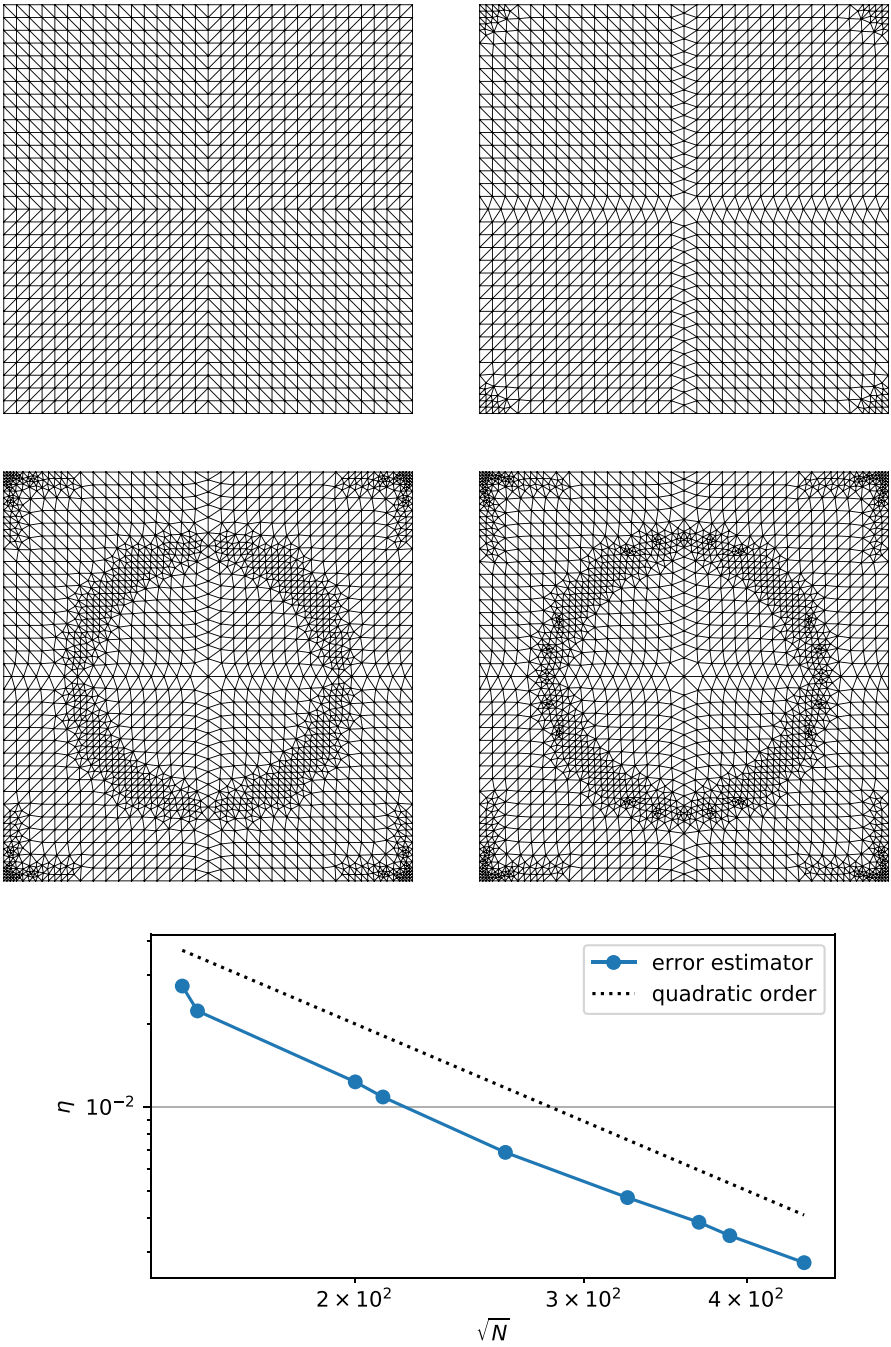

Fig. 5 Some examples from the sequence of adaptively refined meshes for the square problem, and the total error estimator η

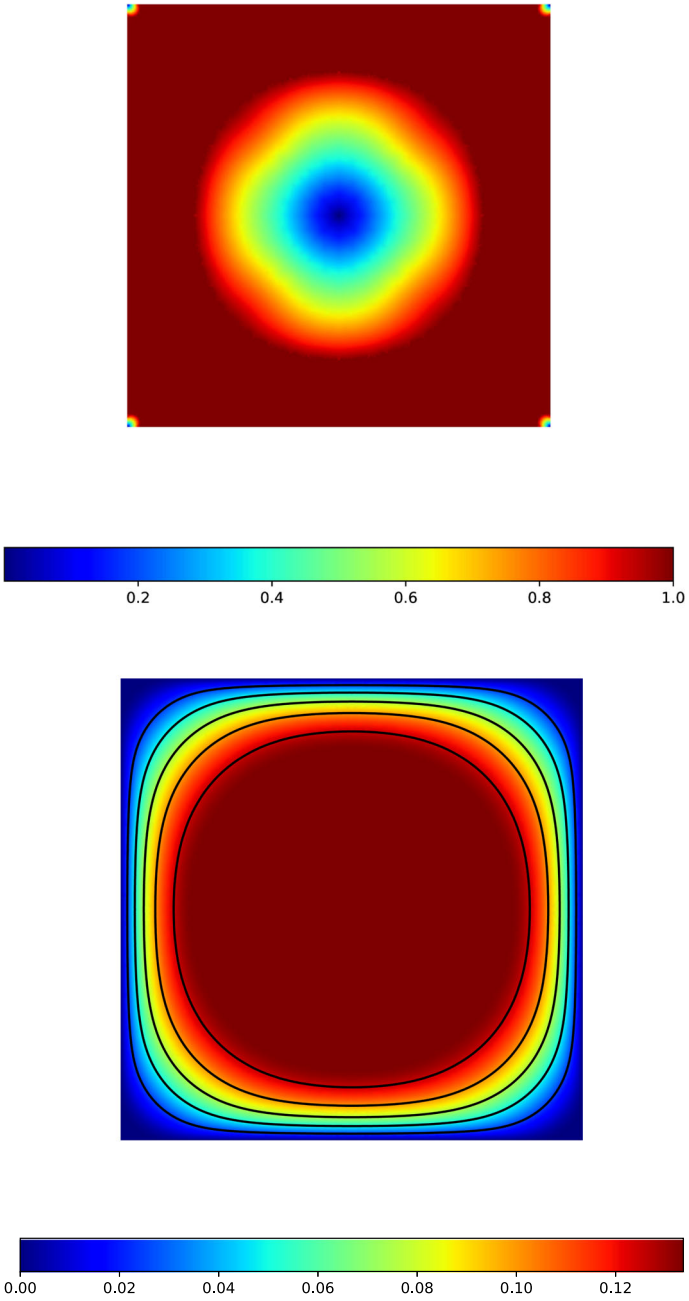

Fig. 6 The length of the discrete Lagrange multiplier $|\boldsymbol{\lambda}_h|$ and the discrete velocity u_h for the square problem

Acknowledgements The numerical results (see [22] for source code) were created using scikit-fem [23] which relies heavily on NumPy [24], SciPy [25] and Matplotlib [26]. The work was supported by the Academy of Finland (decisions 324611 and 338341).

Funding Open Access funding provided by Aalto University.

References

1. Fuchs, M., Seregin, G.: Variational methods for problems from plasticity theory and for generalized newtonian fluids. Lecture Notes in Mathematics, vol. 1749, p. 269. Springer, Heidelberg (2000). https://doi.org/10.1007/BFb0103751
2. Mosolov, P.P., Miashikov, V.P.: On stagnant flow regions of a viscous-plastic medium in pipes. J. Appl. Math. Mech. **30**(4), 841–854 (1966). https://doi.org/10.1016/0021-8928(66)90035-9
3. Mosolov, P.P., Miasnikov, V.P.: On qualitative singularities of the flow of a viscoplastic medium in pipes. J. Appl. Math. Mech. **31**(3), 609–613 (1967). https://doi.org/10.1016/0021-8928(67)90055-X
4. Huilgol, R.R., Panizza, M.: On the determination of the plug flow region in Bingham fluids through the application of variational inequalities. J. Non-Newt. Fluid Mech. **58**, 207–217 (1995). https://doi.org/10.1016/0377-0257(95)01342-S
5. Balmforth, N.J., Frigaard, I.A., Ovarlez, G.: Yielding to stress: recent developments in viscoplastic fluid mechanics. In: Annual review of fluid mechanics. Vol. 46. Annu. Rev. Fluid Mech., vol. 46, pp. 121– 146. Annual Reviews, Palo Alto, CA (2014). https://doi.org/10.1146/annurev-fluid-010313-141424
6. Duvaut, G., Lions, J.-L.: Inequalities in Mechanics and Physics. Grundlehren der Mathematischen Wissenschaften, vol. 219, p. 397. Springer, Heidelberg (1976). https://doi.org/10.1007/978-3-642-66165-5
7. Glowinski, R.: Numerical methods for nonlinear variational problems. Springer Series in Computational physics, p. 493. Springer, New York (1984). https://doi.org/10.1007/978-3-662-12613-4
8. He, J.W., Glowinski, R.: Steady Bingham fluid flow in cylindrical pipes: a time dependent approach to the iterative solution. Numer. Lin. Algeb. Appl. **7**, 381–428 (2000). https://doi.org/10.1002/1099-1506(200009)7:6<381::AID-NLA203>3.0.CO;2-W
9. Glowinski, R.: Sur l'approximation d'une inéquation variationnelle elliptique de type Bingham. R. A. I. R. O. Analyse numérique **10**(R-3), 13–30 (1976)
10. Carstensen, C., Reddy, B.D., Schedensack, M.: A natural nonconforming FEM for the Bingham flow problem is quasi-optimal. Numerische Mathematik **133**(1), 37–66 (2016). https://doi.org/10.1007/s00211-015-0738-1
11. Falk, R.S., Mercier, B.: Error estimates for elasto-plastic problems. RAIRO Analyse Numérique **11**(2), 135–144219 (1977). https://doi.org/10.1051/m2an/1977110201351
12. Roquet, N., Saramito, P.: An adaptive finite element method for Bingham fluid flows around a cylinder. Comp. Meth. Appl. Mech. Eng. **192**(31–32), 3317–3341 (2003). https://doi.org/10.1016/S0045-7825(03)00262-7
13. Cascavita, K.L., Bleyer, J., Chateau, X., Ern, A.: Hybrid discretization methods with adaptive yield surface detection for Bingham pipe flows. J. Scient. Comp. **77**(3), 1424–1443 (2018). https://doi.org/10.1007/s10915-018-0745-3
14. Hage, D., Klein, N., Suttmeier, F.T.: Adaptive finite elements for a certain class of variational inequalities of second kind. Calcolo **48**(4), 293–305 (2011). https://doi.org/10.1007/s10092-011-0040-2

15. Gustafsson, T., Stenberg, R., Videman, J.: Mixed and stabilized finite element methods for the obstacle problem. SIAM J. Numer. Anal. **55**(6), 2718–2744 (2017). https://doi.org/10.1137/16M1065422
16. Stenberg, R.: A technique for analysing finite element methods for viscous incompressible flow. **11**, 935–948 (1990). The Seventh international conference on finite elements in flow problems (Huntsville, AL, 1989) https://doi.org/10.1002/fld.1650110615
17. Clément, P.: Approximation by finite element functions using local regularization. RAIRO Analyse Numérique **9**(R–2), 77–84 (1975)
18. Girault, V., Raviart, P.-A.: Finite element methods for Navier–Stokes equations. Springer series in computational mathematics, vol. 5, p. 374. Springer, Heidelberg (1986). Theory and algorithms https://doi.org/10.1007/978-3-642-61623-5
19. Carstensen, C.: Clément interpolation and its role in adaptive finite element error control. In: Partial differential equations and functional analysis. Operator theory: advances and applications, vol. 168, pp. 27– 43. Birkhäuser, Basel (2006). https://doi.org/10.1007/3-7643-7601-5_2
20. Braess, D.: Finite Elemente - Theorie. Schnelle Löser und Anwendungen in der Elastizitätstheorie. Springer, Heidelberg (2013)
21. Saramito, P., Roquet, N.: An adaptive finite element method for viscoplastic fluid flows in pipes. Comp. Meth. Appl. Mech. Eng. **190**(40–41), 5391–5412 (2001). https://doi.org/10.1016/S0045-7825(01)00175-X
22. Gustafsson, T.: Source code for the numerical experiments: kinnala/paper-bingham (2022). https://doi.org/10.5281/zenodo.6572862
23. Gustafsson, T., McBain, G.D.: scikit-fem: a python package for finite element assembly. J. Open Sour. Softw. **5**(52), 2369 (2020). https://doi.org/10.21105/joss.02369
24. Harris, C.R., Millman, K.J., Van Der Walt, S.J., Gommers, R., Virtanen, P., Cournapeau, D., Wieser, E., Taylor, J., Berg, S., Smith, N.J., et al.: Array programming with NumPy. Nature **585**(7825), 357–362 (2020). https://doi.org/10.1038/s41586-020-2649-2
25. Virtanen, P., Gommers, R., Oliphant, T.E., Haberland, M., Reddy, T., Cournapeau, D., Burovski, E., Peterson, P., Weckesser, W., Bright, J., et al.: SciPy 10: fundamental algorithms for scientific computing in Python. Nat. Meth. **17**(3), 261–272 (2020). https://doi.org/10.1038/s41592-019-0686-2
26. Hunter, J.D.: Matplotlib: a 2d graphics environment. Comp. Sci. & Eng. **9**(03), 90–95 (2007). https://doi.org/10.1109/MCSE.2007.55